Dynamically downscaled Mk3.0 climate projection for the Marine and Tropical Sciences Research Facility (MTSRF) from 2060-2090

Marcus Thatcher and John McGregor
28 February 2008

Report prepared for the Marine and Tropical Sciences Research Facility

[Insert: ISBN and Cataloguing-in-Publication (CIP) information here:]

For an ISBN number, or ISSN number (an ISSN only applies if the report is part of an ongoing series), contact Louise.Bell@csiro.au or Lea.Crosswell@csiro.au

Allow 10 working days from submitting your application to the National Library to receipt of your CIP information.

Enquiries should be addressed to:

Dr Marcus Thatcher
CSIRO Marine and Atmospheric Research
107 Station Street. Aspendale. VIC

Distribution list

Chief of Division

Operations Manager

Project Manager

Client

Authors

Other CSIRO Staff

National Library

CMAR Libraries

Important Notice

Use of this Report

The use of this Report is subject to the terms on which it was prepared by CSIRO. In particular, the Report may only be used for the following purposes.

- this Report may be copied for distribution within the Client's organisation;
- the information in this Report may be used by the entity for which it was prepared ("the Client"), or by the Client's contractors and agents, for the Client's internal business operations (but not licensing to third parties);
- extracts of the Report distributed for these purposes must clearly note that the extract is part of a larger Report prepared by CSIRO for the Client.

The Report must not be used as a means of endorsement without the prior written consent of CSIRO.

The name, trade mark or logo of CSIRO must not be used without the prior written consent of CSIRO.

CONTENTS

1. INTRODUCTION

Coupled ocean-atmosphere Global Climate Models (GCMs) represent one of our most effective tools for exploring the response of our environment to various GreenHouse Gas (GHG) emission scenarios. For example, the outputs of GCMs are typically used to make projections of future climate change (CSIRO, 2007), and are used to plan adaptation and mitigation strategies. However, due to the complexity of the coupled atmosphere-ocean-land surface system, most GCMs operate at relatively low spatial resolution (e.g., typically between 2 and 5 degrees or approximately 220 km to 560 km) and therefore do not provide sufficient spatial detail to understand regional scale changes in climate that are induced by global warming.

To produce regional climate change projections, it is necessary to apply downscaling techniques to the GCM output. In the case of dynamical downscaling, Regional Climate Models (RCMs) simulate atmospheric dynamics and physics using modelling techniques that are similar to those used in GCM's, but with enhancements for simulating meso-scale and local-scale meteorology. To account for surface forcings that influence the local climate, RCMs employ higher resolution surface datatsets (e.g., orography, land-use, albedo, etc). Most RCMs also assimilate some features of the large-scale synoptic weather patterns and global warming trends from the host GCM into their simulations. In this way, RCMs are designed to dynamically respond to changes in climate like GCMs, while providing much higher spatial resolution for regional climate projections.

To make climate change projections for Australia, CSIRO has developed the Mk3.0 coupled ocean-atmosphere GCM (Gordon, et. al, 2002) and the Conformal Cubic Atmospheric Model (CCAM) (McGregor, 2005, McGregor and Dix, 2008). Typically these two models are used together, with Mk3.0 simulating the global climate and CCAM dynamically downscaling the Mk3.0 output to regional scales. This is possible because CCAM is an Atmospheric Global Climate Model (AGCM) that employs a stretched global grid which can be focused for regional climate applications. CCAM is also computationally efficient due to its semi-implicit, semi-Lagrangian formulation, which allows the regional climate simulation to be completed within a practical amount of time (e.g., weeks instead of months or years).

In this report, we describe the results of a 2060-2090 regional climate projection over the tropical rainforest region of northern Queensland, assuming an A2 emission scenario (IPCC, 2007). The global climate was simulated using Mk3.0 at approximately 200 km resolution and then dynamically downscaled to 15 km resolution using CCAM. Regional climate projections for the average daily maximum (screen) temperature, average daily minimum (screen) temperature and average daily rainfall are made for each season relative to the results of the previous CCAM control run (Thatcher, McGregor and Nguyen, 2007). The statistical significance of projected changes in regional climate is estimated from the simulated interdecadal variability. We also compare probability distributions of maximum temperature, minimum temperature and rainfall between the 1970-2000 control run and the 2060-2090 climate projection. The resultant regional climate projection datasets can be used to study various climate change impacts, such as the implications for hydrology.

2. SIMULATION METHODOLOGY

The conformal cubic grid used by CCAM can be conceptually visualised by taking a grid on the surface of a cube, and then projecting the cube onto a sphere (see Fig. 1).

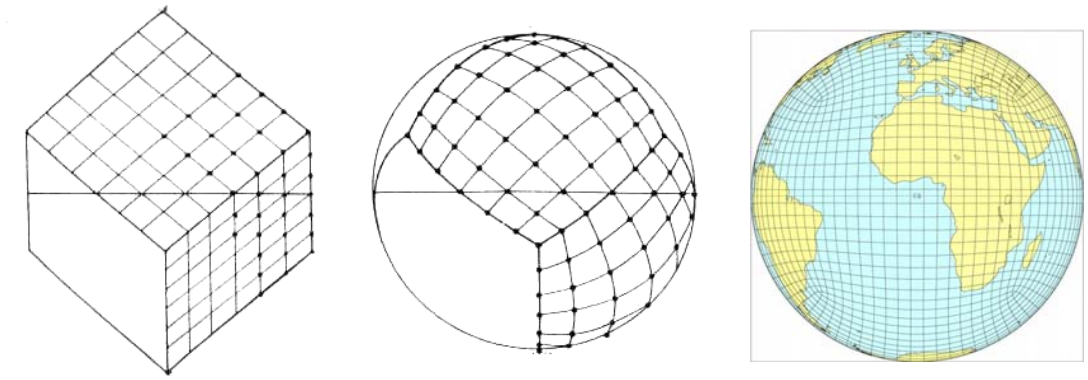

Figure 1: Schematic representation of the conformal cubic grid and its projection on the surface of a sphere.

Note that the region of interest (e.g., northern Queensland for this study) is located at the centre of a cubic panel. For the experiments described in this report, we use a C48 grid with 18 vertical levels (using normalised pressure coordinates known as sigma levels). The C48 grid indicates that 48x48 grid points are used for each cubic panel, resulting in 6x48x48 horizontal grid points for the entire globe. The lowest and highest vertical levels are approximately 40 m and 35 km, respectively, with screen wind speeds (10 m) and screen temperatures (2 m) being calculated using a technique described by McGregor et al. (1993) which is based on Monin-Obukhov similarity theory. This vertical and horizontal configuration of CCAM has been optimised to obtain accurate results in a reasonable amount of time.

The conformal cubic grid can be stretched to provide a regional focus using a Schmidt transformation (Schmidt, 1977). The amount of stretching is controlled by the Schmidt factor, S, where higher values of S indicate greater amounts of stretching (i.e., finer resolution). A value of S=1 denotes no stretching. For example, S=3.3 results in a conformal cubic grid with approximately 60 km resolution over Australia (see Fig. 2).

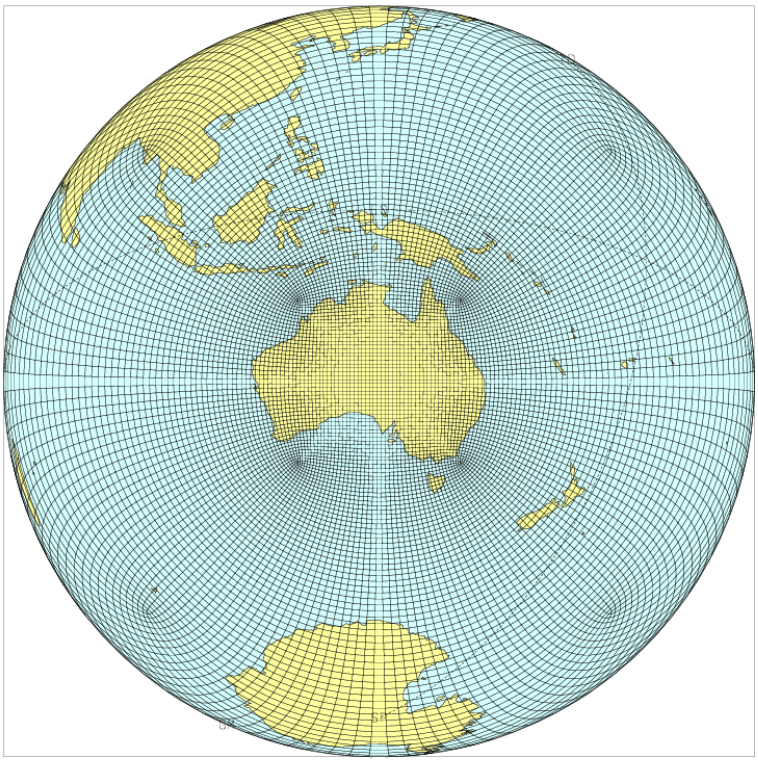

Figure 2: Example of the conformal cubic grid with *S*=3.3, resulting in an approximately 60 km resolution grid over Australia.

For the experiment described in this report, we use CSIRO's Mk3.0 GCM to simulate the future global climate at 200 km resolution assuming an A2 emission scenario. The A2 emission scenario is reasonably consistent with current trends in GHG emissions. The Mk3.0 output is dynamically downscaled to 15 km by CCAM using a multiple one-way nesting approach, where Mk3.0 output is first downscaled to 60 km resolution using *S*=3.3 (see Fig. 2). The output of the CCAM 60 km simulation is then downscaled a second time by CCAM to 15 km resolution using *S*=16.7 (see Fig. 3). This two step process is used because the boundary condition data provided by Mk3.0 is too coarse to be used directly with the highly stretched 15 km conformal cubic grid. Note that in the case of CCAM there is no need for two-way nesting since the stretched global grid accounts for the feedback between the high resolution region and the lower resolution host data.

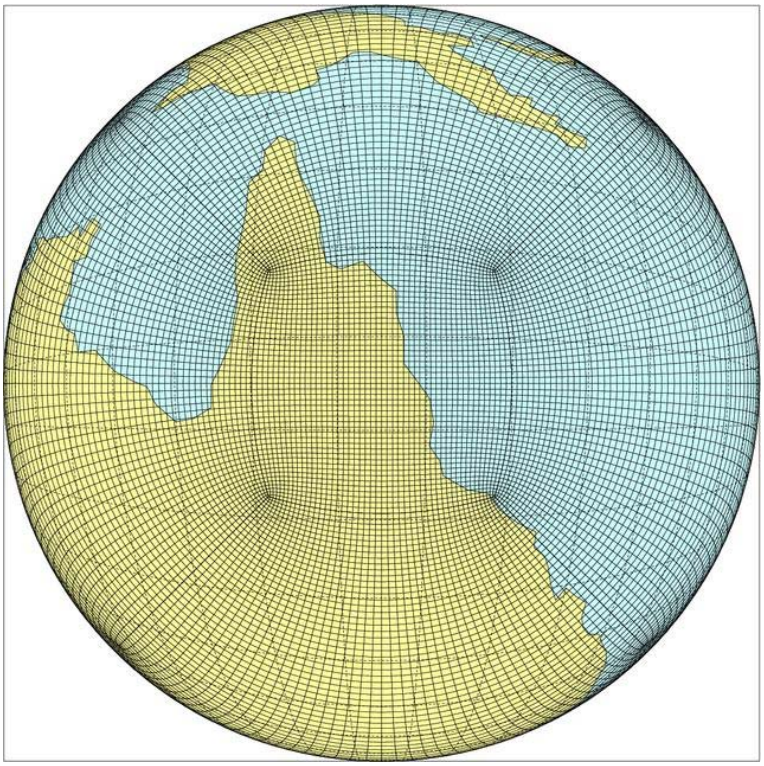

Figure 3: Example of the conformal cubic grid with S=16.7, resulting in an approximately 15 km resolution grid over the MTSRF region in northern Queensland.

The downscaling of Mk3.0 output to 60 km resolution by CCAM was performed by Nguyen and McGregor (2008). For the 60 km CCAM simulation they used the Sea Surface Temperatures (SSTs) from the Mk 3.0 output, after first subtracting present-day monthly-averaged biases. The broad-scale upper level winds (i.e., above 500 hPa) and the surface pressure were assimilated from Mk3.0 using a scale-selective filter (Thatcher and McGregor, 2008). The scale-selective filter was used since it is far more effective at assimilating host model data into CCAM compared to boundary value nudging techniques (i.e., the scale-selective filter perturbs all grid points, not just at the boundaries). A filter diameter of approximately 30 degrees was used for the 60 km simulation and applied once every six hours.

The scale-selective filter is also used to assimilate the atmospheric data from the 60 km simulation into the CCAM 15 km simulation. In this case we assimilate the winds, air temperature and mixing ratio above 900 hPa, as well as the surface pressure. For the 15 km simulation we use a filter diameter of approximately 8 degrees and apply the filter once every six hours.

CCAM employs a cumulus convection scheme developed by McGregor (2003), an implicit cloud microphysics scheme devised by Rotstayn (1997) and a canopy scheme developed by Kowalczyk (1994) which includes six layers for soil temperature and soil moisture. Longwave and shortwave radiation is determined by the GFDL parameterisation (Schwarzkopf and Fels, 1991) and the gravity wave drag scheme is implemented according to Chouinard, et al. (1986). CCAM employs a stability dependent boundary layer scheme (McGregor et al. 1993) combined with non-local vertical mixing (Holtslag and Boville, 1993) and an enhanced mixing of cloudy boundary layer air (Smith, 1990). Orography data is obtained from 250 m resolution datasets created by Geoscience Australia and surface land-use is estimated from the Graetz 6 km resolution dataset for Australia ().

It is not possible to account for uncertainties arising from the GCM simulation or emission scenario using a single A2, Mk3.0 experiment. However, we can still quantify the statistical significance of predicted changes in climate relative to the simulated climate variability. Specifically we use Student's t-distribution to estimate the 95% confidence interval of changes in rainfall, daily maximum screen temperature and daily minimum screen temperatures. In this way, the errors quantified in this report are essentially dependent on the interdecadal climate variability as simulated by CCAM.

3. SIMULATION RESULTS

In this report we measure regional climate change in terms of the average difference between the projected 2060-2090 climate and the simulated 1970-2000 climate from the CCAM control run (i.e., a relative measure of climate change). The spatial dependence of the average simulated climate change is compared to the observed climatology for 1960-2000, as published by the Australian Bureau of Meteorology. We also estimate the 95% confidence interval for the mean climate change using a Student t-distribution. Note that the confidence interval is derived from the simulated climate variability and does not take into account GCM or emission scenario uncertainties.

3.1 Predicted changes in average daily maximum screen temperature

When considering northern Queensland, it is appropriate to consider the predicted changes in climate in terms of the transitional season #1 (November to December), the wet season (January to March), transitional season #2 (April to July) and the dry season (August to October). In Fig. 4 we plot the projected regional climate change for the average maximum screen temperature (between 2060-2090 and 1970-2000), for each of the above seasons. For comparison Fig. 5 shows the average maximum temperatures for the same seasons as measured by the Australian Bureau of Meteorology (1960-2000).

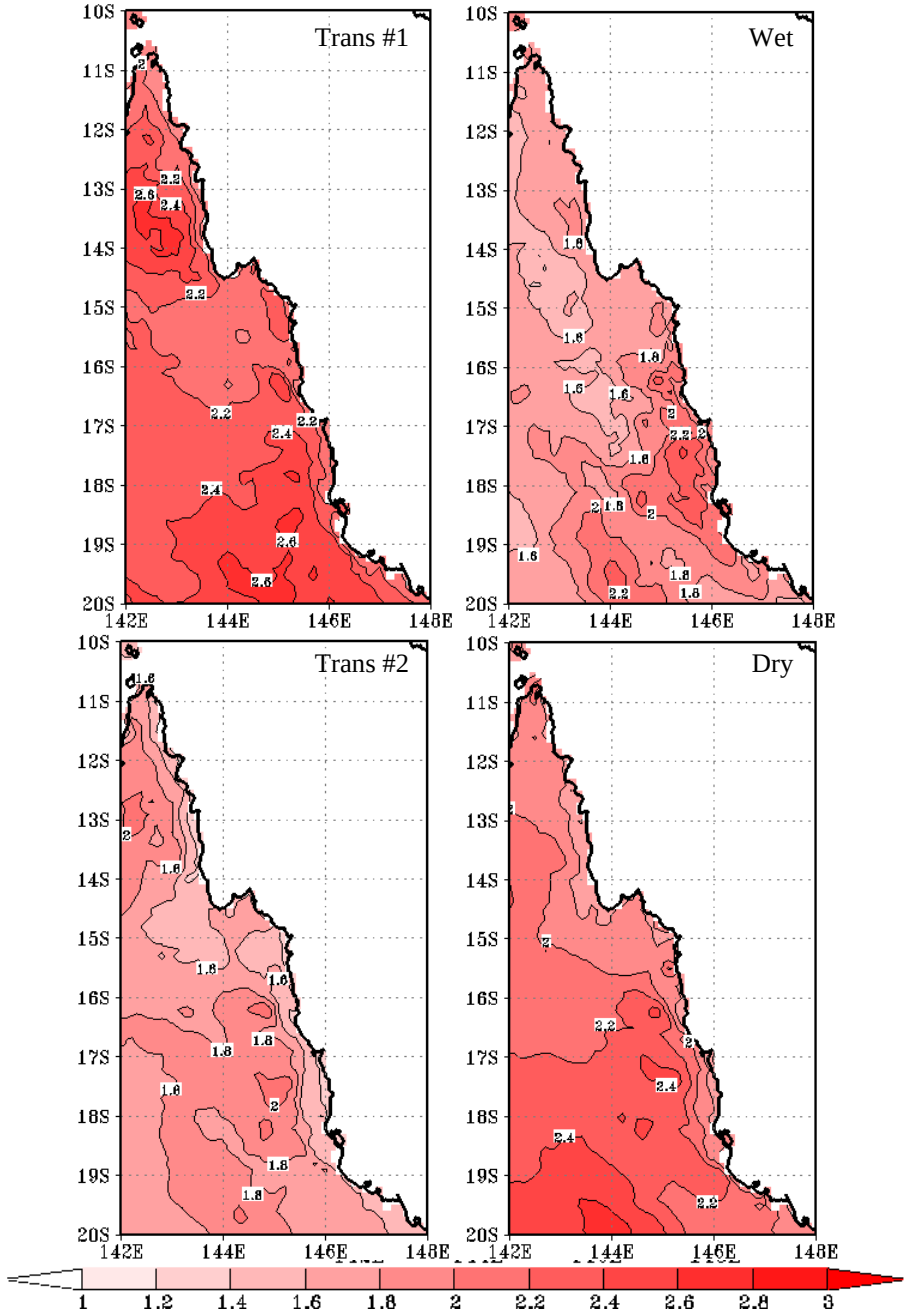

Figure 4: Projected change in average daily maximum screen temperature between 1970-2000 and 2060-2090, for transitional season #1 (top left), wet season (top right), transitional season #2 (bottom left) and dry season (bottom right). Units are degrees Celsius in all figures.

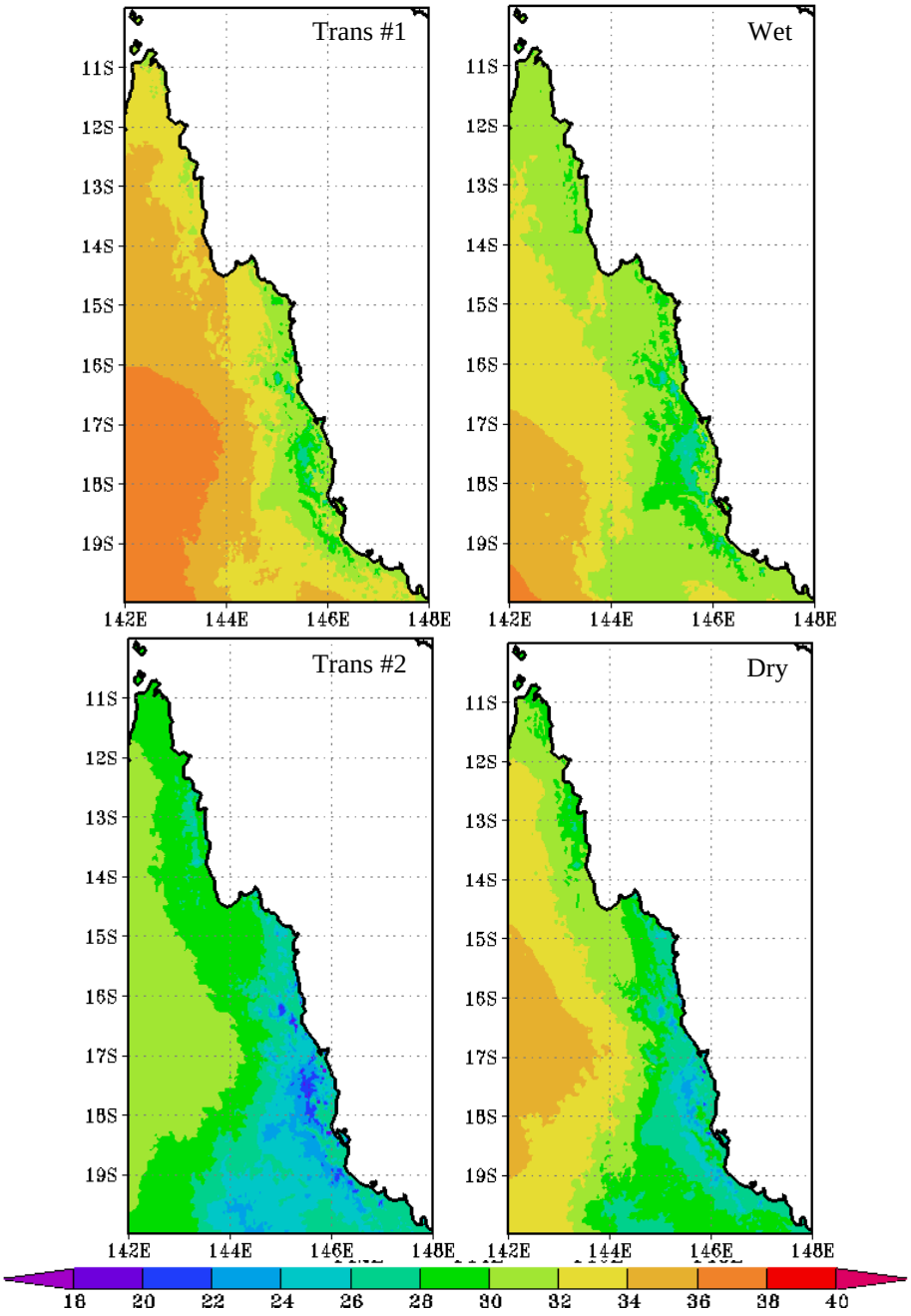

Figure 5: Observed 1961-1990 average daily maximum temperature as measured by the Australian Bureau of Meteorology for transitional season #1 (top left), wet season (top right), transitional season #2 (bottom left) and dry season (bottom right). Units are degrees Celsius in all figures.

The simulated future climate suggests that the daily maximum screen temperature will increase by approximately 1.6 to 2.6 degrees on average, with the increase showing a complex spatial dependence. The uncertainty in the predicted increase due to the simulated climate variability is estimated using a Student t-distribution at the 95% confidence level, as shown in Fig. 6. Since the size of the predicted increase in daily maximum temperature shown in Fig. 4 is greater than the uncertainty due to climate variability shown in Fig. 6, then the simulated increase is statistically significant in this experiment. Note that the simulation produces a larger increase in the average daily maximum screen temperature for transitional season #1 and the dry season, compared to the other seasons. Typically the increases in maximum temperature tend to be greater in the southern part of the domain compared to the northern part.

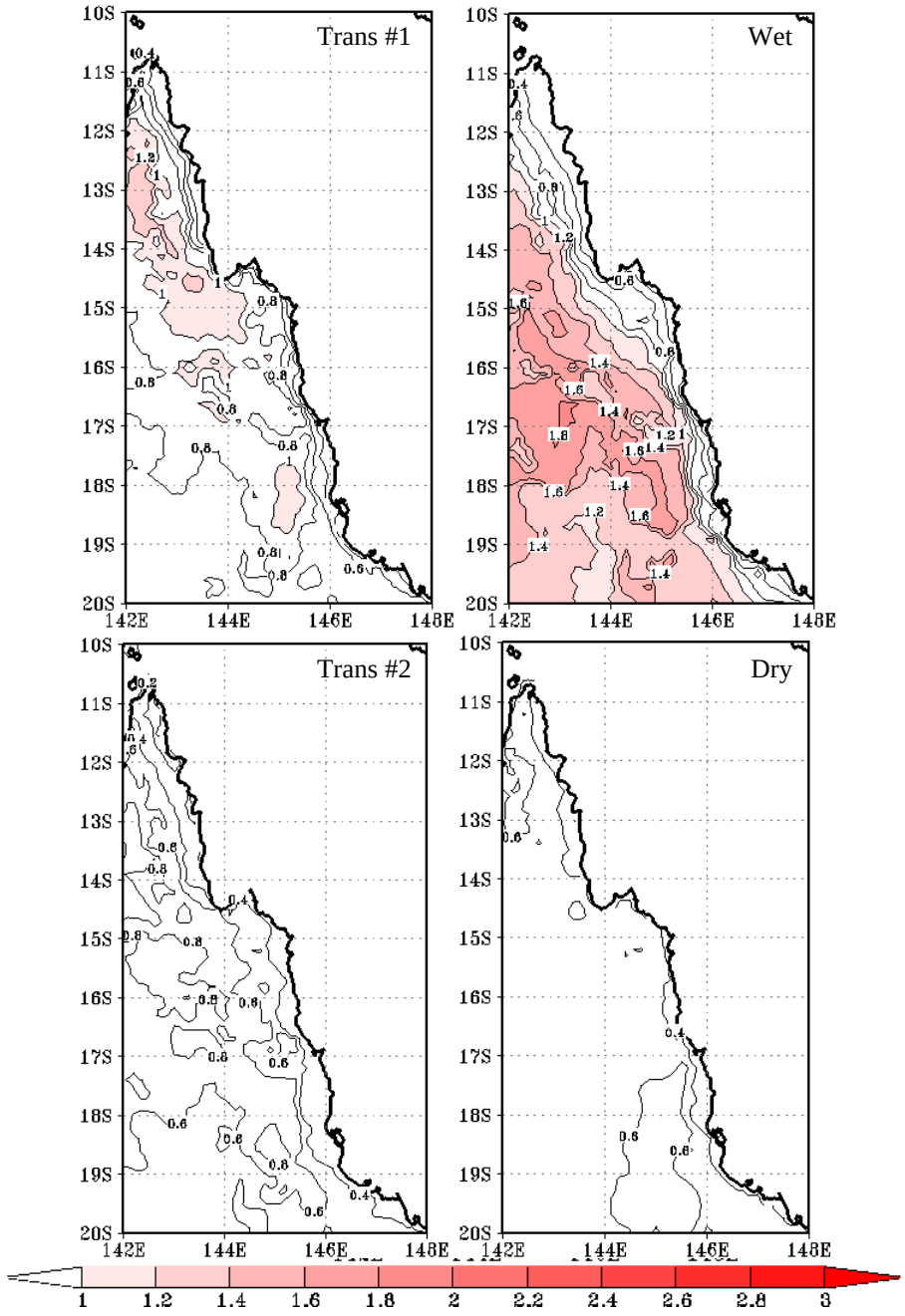

Figure 6: 95% confidence interval for the average daily maximum screen temperature (as estimated from the simulated climate variability) for transitional season #1 (top left), wet season (top right), transitional season #2 (bottom left) and dry season (bottom right). Units are degrees Celsius in all figures.

Further insight into the projected change in maximum screen temperature can be obtained from Fig. 7, where we compare the probability distribution functions (PDFs) between the 1970-2000 control run and the 2060-2090 simulated climate for the grid box containing Cairns (16.9S, 145.7E). Note that for this simulation we have not included local urban influences such as anthropogenic heat fluxes from traffic, which can increase the temperature relative to the surrounding rural areas.

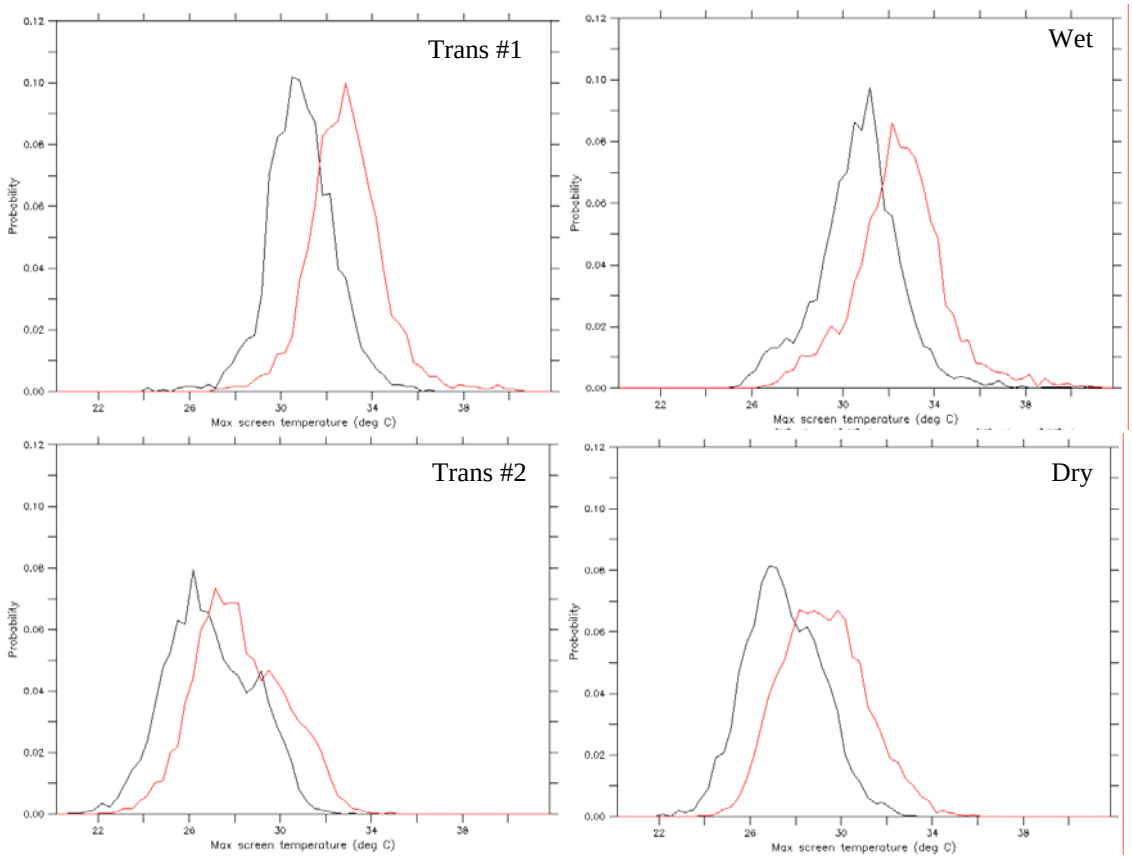

Figure 7: Maximum screen temperature probability distribution functions (PDFs) for Cairns (neglecting local urban influences). The 1970-2000 simulated climate is shown as black and the 2060-2090 simulated climate is indicated by red. The PDFs are separated into transitional season #1 (top left), wet season (top right), transitional season #2 (bottom left) and dry season (bottom right).

As previously indicated in Fig. 6, the shift in the maximum temperature PDFs between 1970-2000 and 2060-2090 towards higher temperatures is statistically significant. Interestingly, there does not appear to be any significant change in the shape of the PDFs between the 1970-2000 and 2060-2090 simulated climate.

3.2 Predicted changes in average daily minimum screen temperature

Figure 8 shows the corresponding predicted increase in average daily minimum screen temperature between 1970-2000 and 2060-2090 (A2 emission scenario), for the same seasons as used in Fig. 4. For comparison, the average observed minimum temperatures (provided by the Bureau of Meteorology), are shown in Fig. 9.

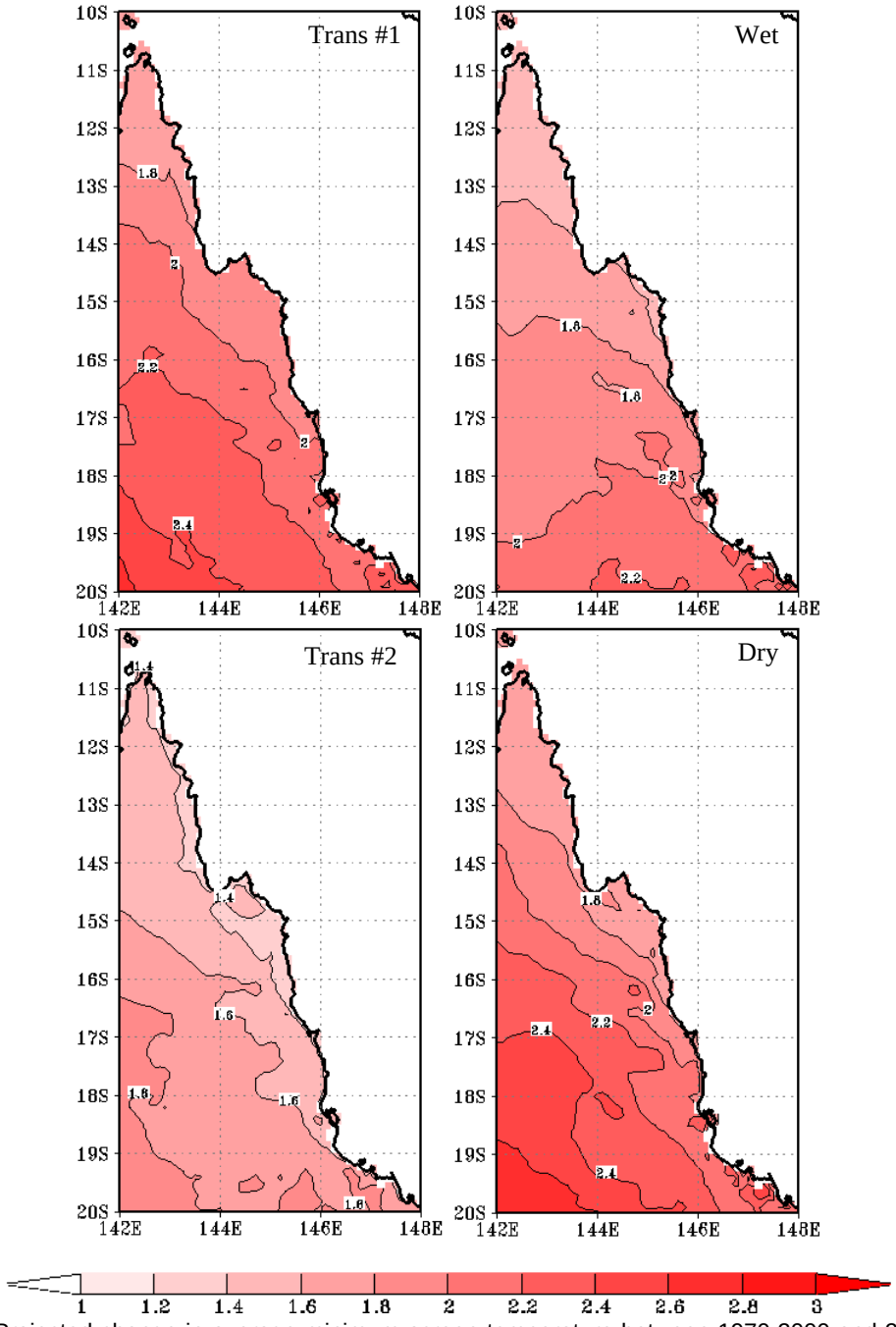

Figure 8: Projected change in average minimum screen temperature between 1970-2000 and 2060-2090, for transitional season #1 (top left), wet season (top right), transitional season #2 (bottom left) and dry season (bottom right). Units are degrees Celsius in all figures.

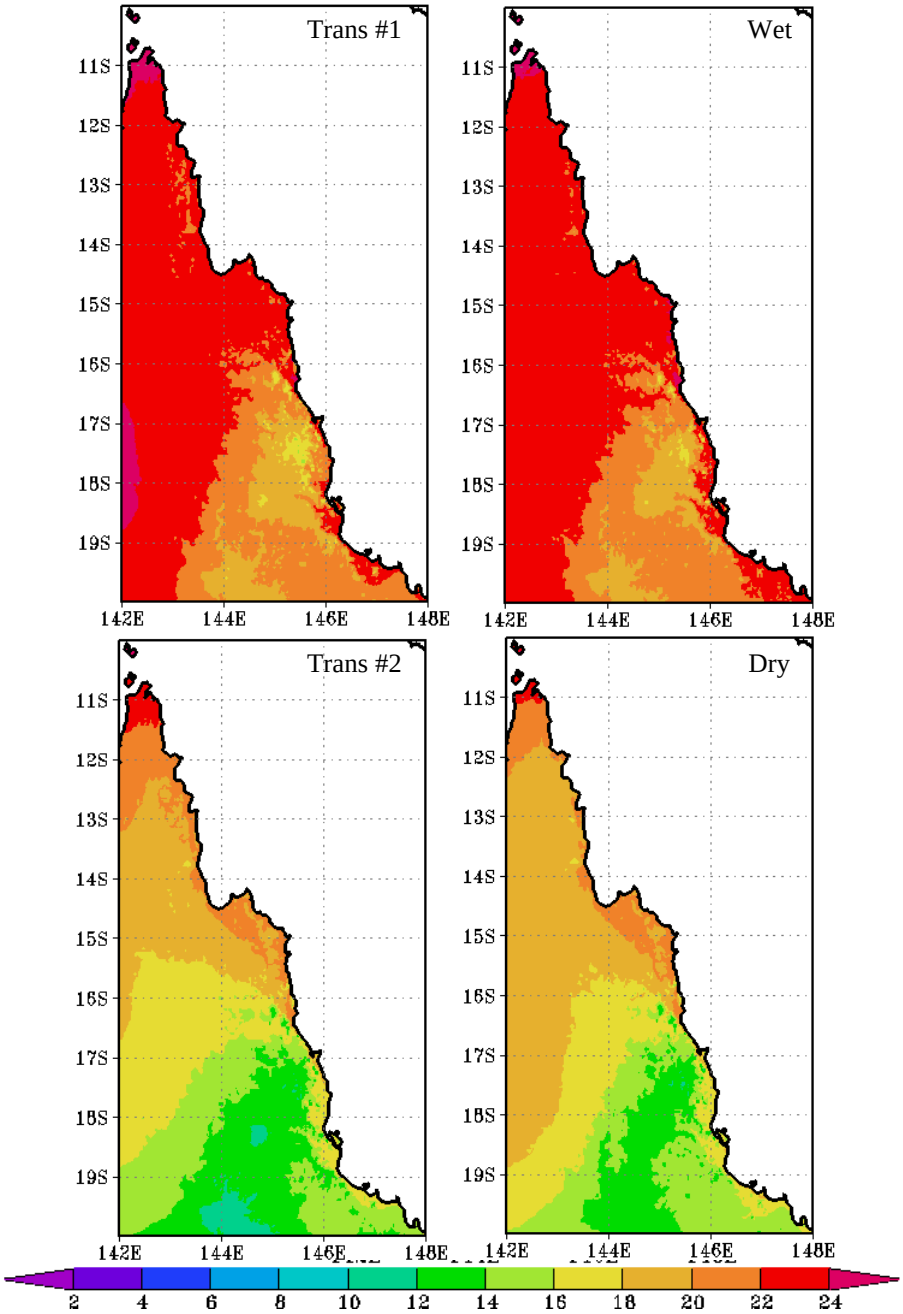

Figure 9: Observed 1960-2000 average minimum temperature as measured by the Australian Bureau of Meteorology for transitional season #1 (top left), wet season (top right), transitional season #2 (bottom left) and dry season (bottom right). Units are degrees Celsius in all figures.

Figure 8 shows the average minimum temperature is predicted to increase between 1.4 and 2.4 degrees for the A2 emission scenario. Typically the size of the increase is greater towards the south of the domain for all seasons. The predicted average change in minimum temperatures is statistically significant (relative to the simulated variability) for all seasons, as indicated by the 95% confidence interval shown in Fig. 10. Note that simulated variability of the minimum screen temperature is less than that of the maximum temperature, resulting in a correspondingly smaller 95% confidence interval (i.e., the changes in minimum temperatures correspond to a higher level of statistical significance). A larger increase in minimum temperatures occurs for the transitional season #1 and the dry season, compared to the transitional season #2 and the wet season, as is the case for the maximum temperature.

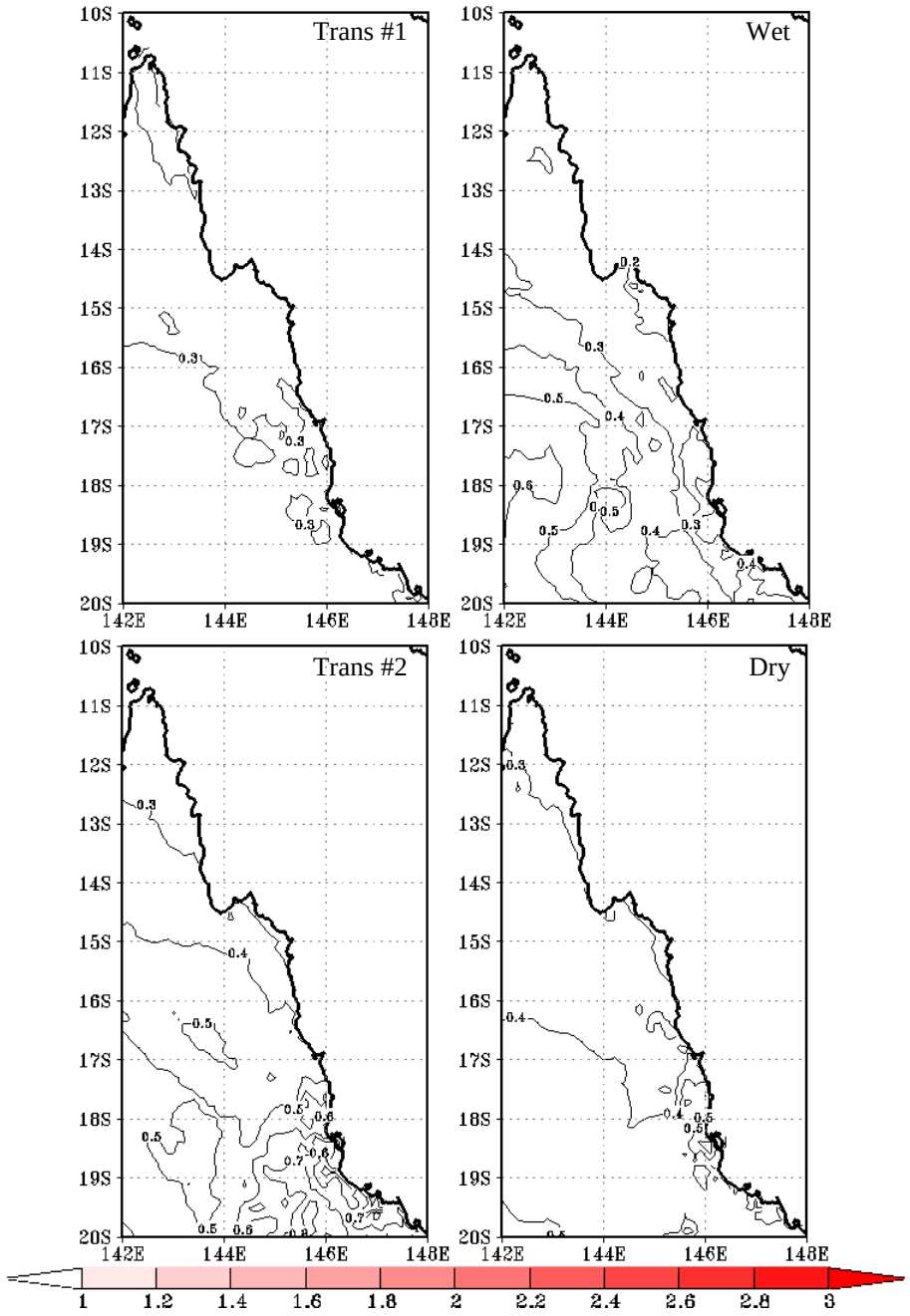

Figure 10: 95% confidence interval for the average minimum screen temperature (as estimated from the simulated climate variability) for transitional season #1 (top left), wet season (top right), transitional season #2 (bottom left) and dry season (bottom right). Units are degrees Celsius in all figures.

A shift in the minimum temperature probability distribution for Cairns is shown in Fig. 11, which is similar to the shift in the probability distribution for maximum temperatures plotted in Fig. 8. No significant change in the shape of the minimum temperature PDFs are predicted between 1970-2000 and 2060-2090.

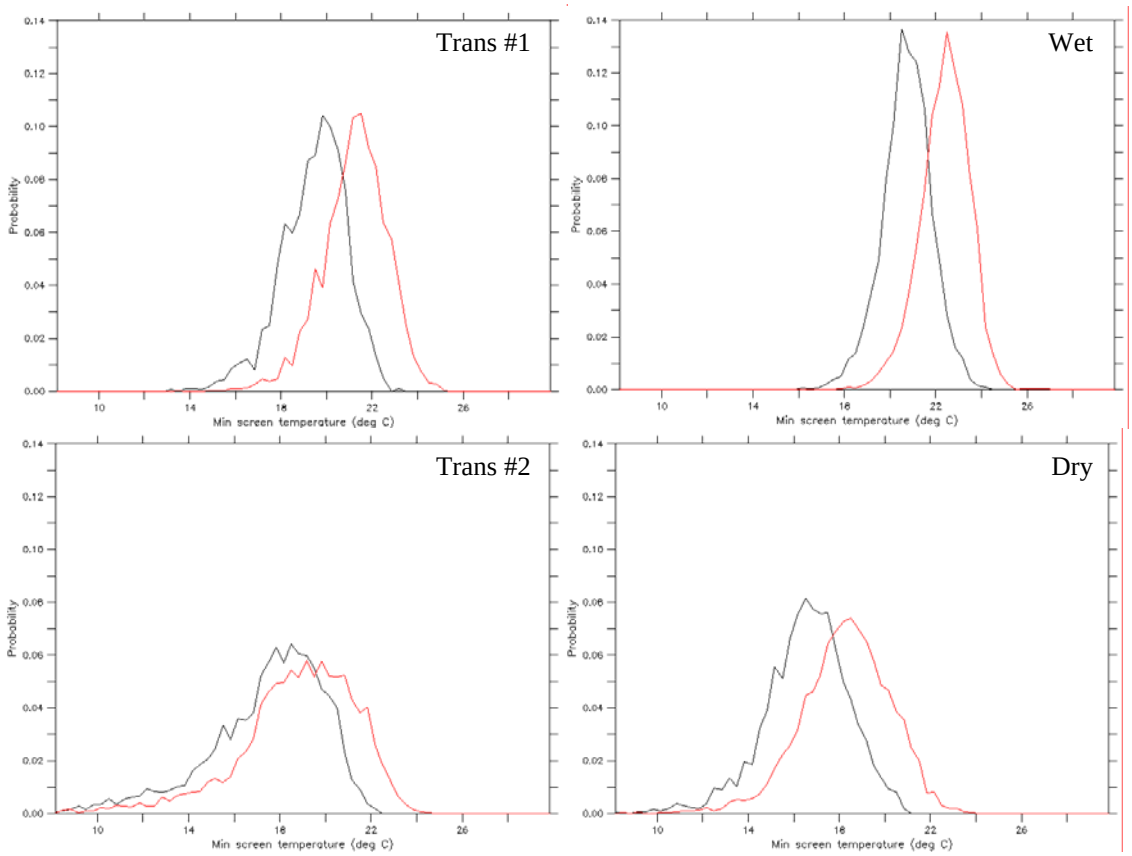

Figure 11: Minimum screen temperature probability distribution functions (PDFs) for Cairns (neglecting local urban influences). The 1970-2000 simulated climate is shown as black and the 2060-2090 simulated climate is indicated by red. The PDFs are separated into transitional season #1 (top left), wet season (top right), transitional season #2 (bottom left) and dry season (bottom right).

3.3 Predicted changes in average daily rainfall

Figure 12 plots the simulated change in average rainfall between 1970-2000 and 2060-2090 for each season, with the current rainfall climatology shown in Fig. 13. Note that none of the simulated changes are statistically significant at the 95% confidence interval (see Fig. 14), compared to the simulated variability in rainfall. Since the uncertainty cannot be a negative value, we use a greyscale shading in Fig. 14 instead of the red/blue shading shown in Fig 13.

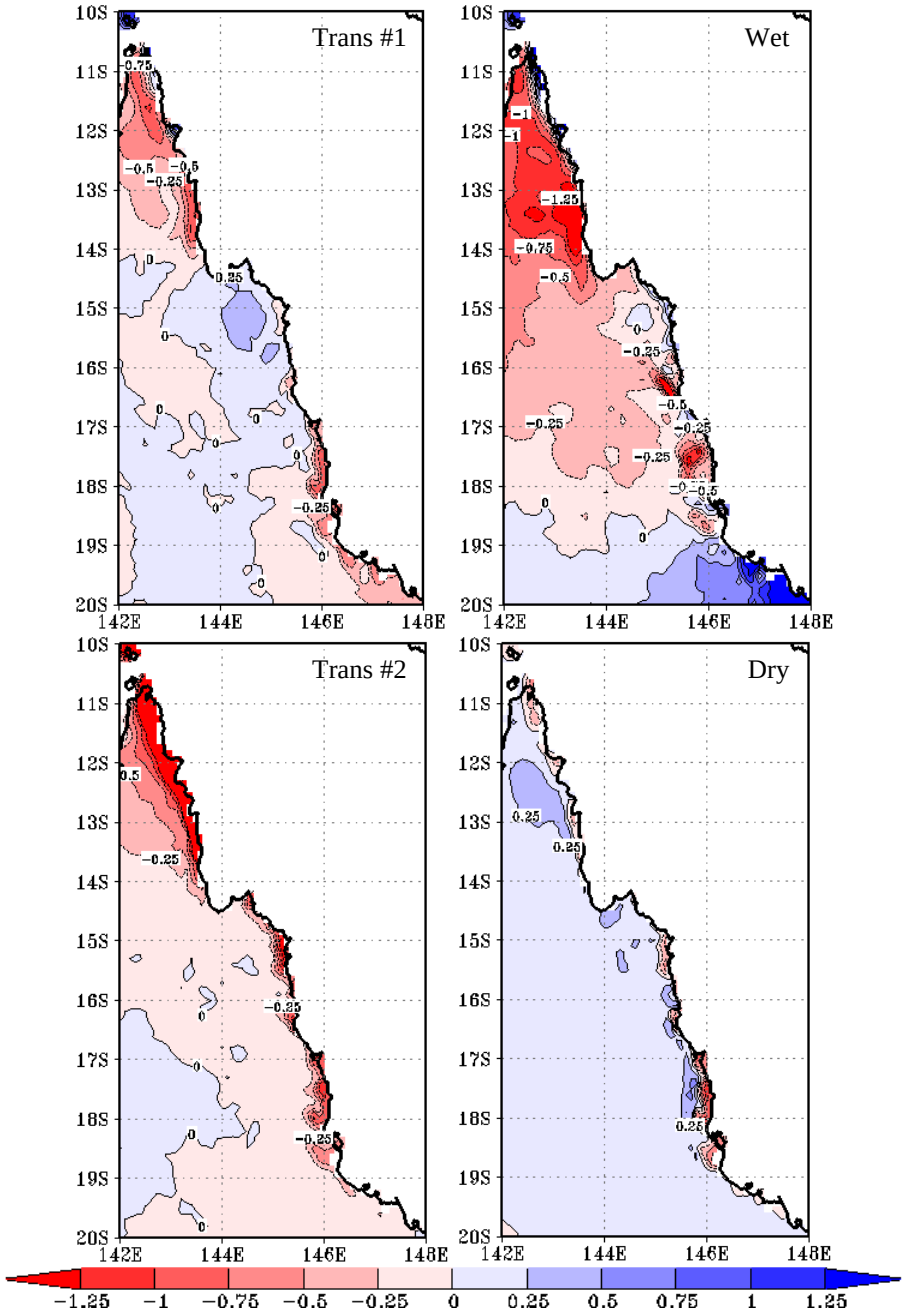

Figure 12: Projected change in average rainfall between 1970-2000 and 2060-2090, for transitional season #1 (top left), wet season (top right), transitional season #2 (bottom left) and dry season (bottom right). Units are mm/day in all figures.

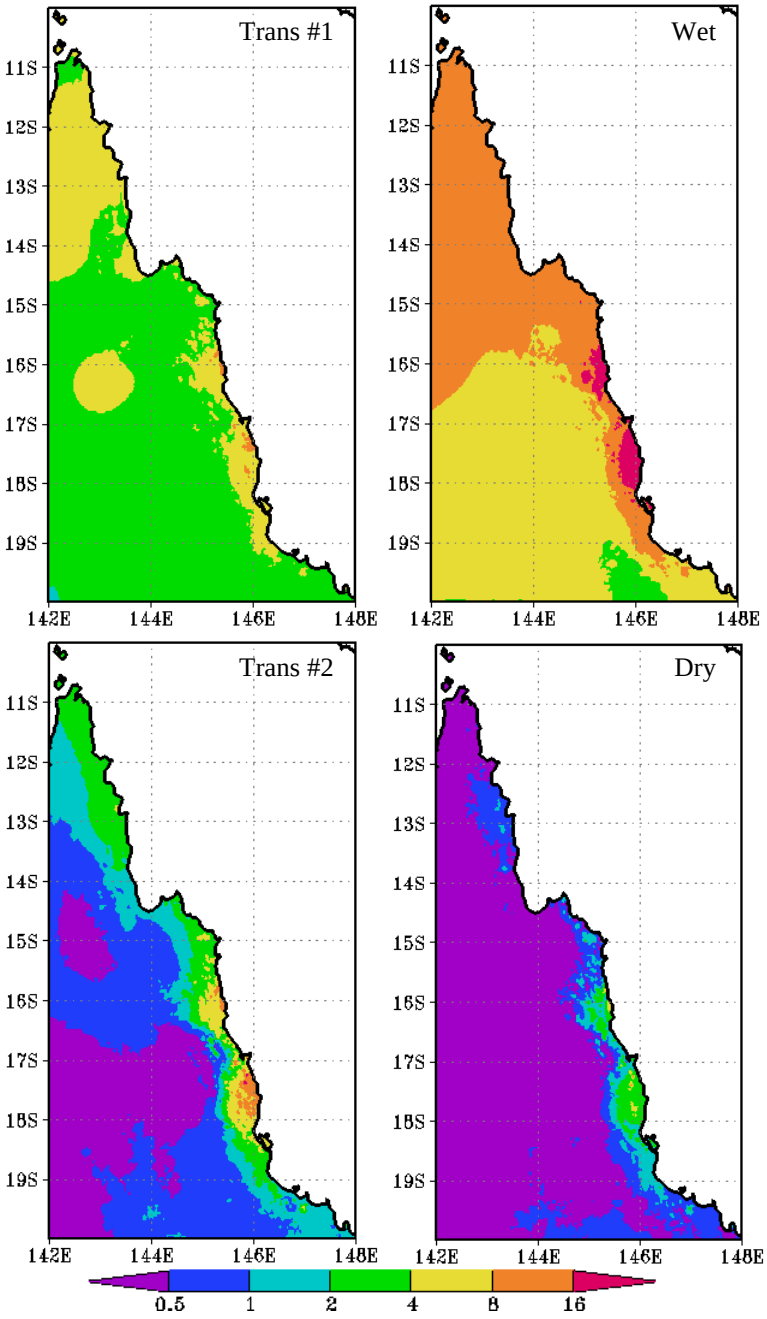

Figure 13: Observed 1960-2000 average rainfall as measured by the Australian Bureau of Meteorology for transitional season #1 (top left), wet season (top right), transitional season #2 (bottom left) and dry season (bottom right). Units are mm/day in all figures.

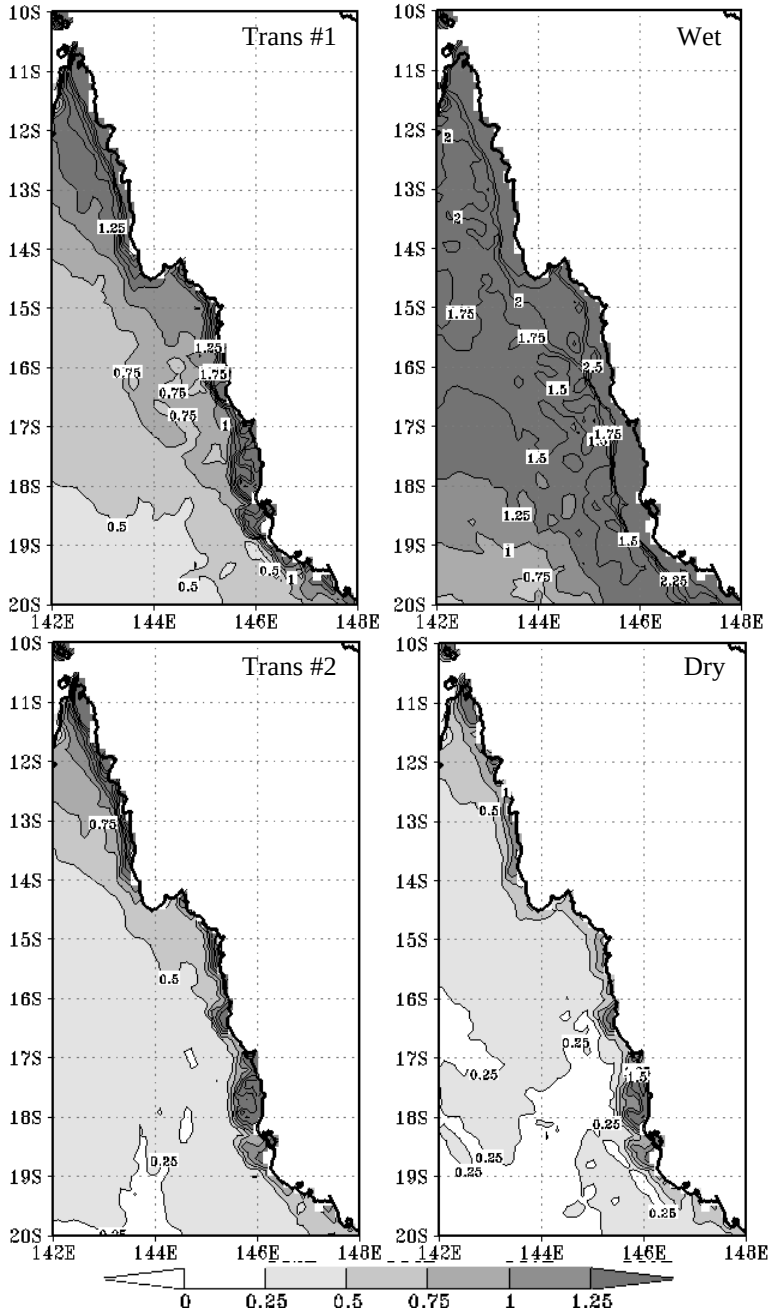

Figure 14: 95% confidence interval for average rainfall change (as estimated from the simulated climate variability) for transitional season #1 (top left), wet season (top right), transitional season #2 (bottom left) and dry season (bottom right). Units are mm/day in all figures.

The lack of any significant change in average rainfall for the A2 emission scenario is clearly apparent in Fig. 15, where we compare the PDFs of simulated rainfall between 1970-2000 and 2060-2090 for Cairns. Nevertheless, the predicted increases in temperatures combined with no comparable increases in rainfall may have important implications for the region.

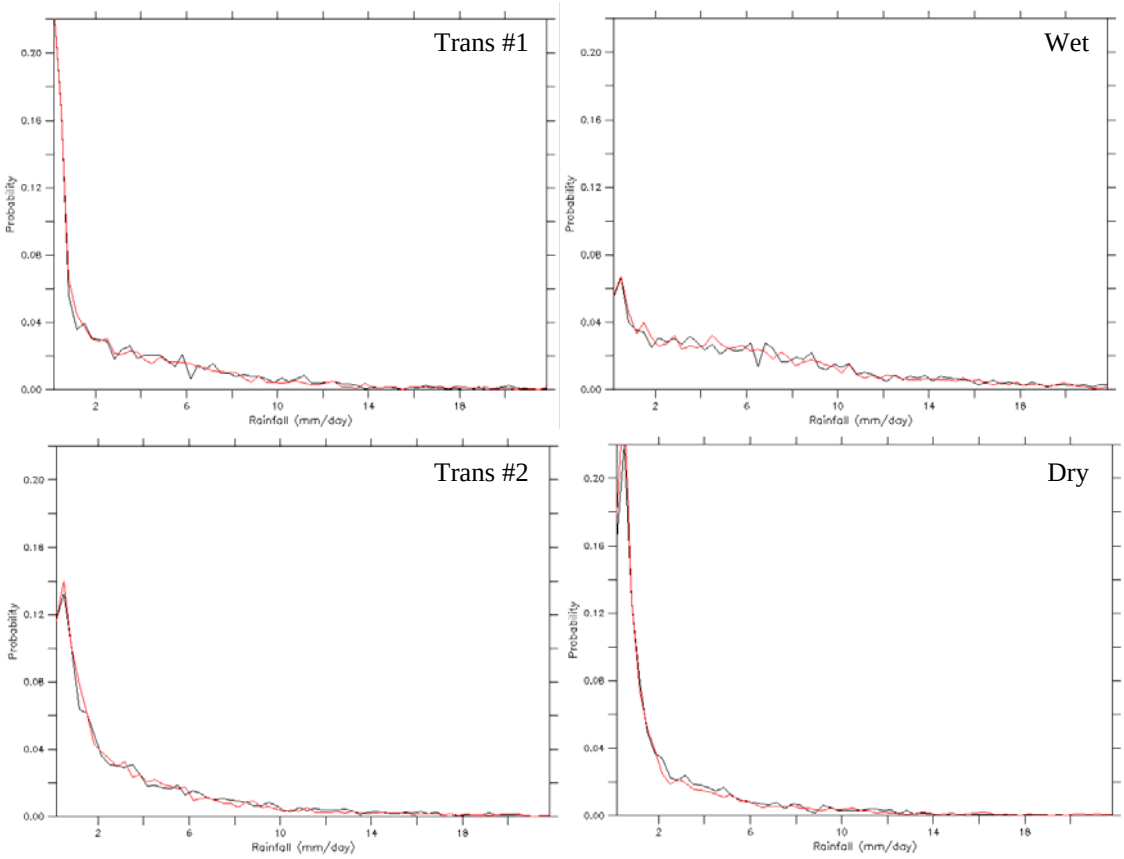

Figure 15: Rainfall probability distribution functions (PDFs) for Cairns (neglecting local urban influences). The 1970-2000 simulated climate is shown as black and the 2060-2090 simulated climate is indicated by red. The PDFs are separated into transitional season #1 (top left), wet season (top right), transitional season #2 (bottom left) and dry season (bottom right).

4. CONCLUSIONS

This report describes regional climate change projections for the MTSRF region of northern Queensland using the A2 emission scenario for 2060-2090. The changes in regional climate were simulated by CCAM at 15 km resolution after dynamically downscaling from Mk3.0 output at 200 km resolution.

Daily minimum screen temperatures are predicted to rise between 1.4 and 2.4 degrees and daily maximum screen temperature between 1.6 and 2.6 degrees on average, depending on the location. There is a tendency for the average increase in minimum temperature to be smaller towards the northern part of the study domain compared to the south. Greater increases in temperature can be expected for transitional season #1 and the dry season, compared to transitional season #2 and the wet season. All changes in average screen temperature are statistically significant at the 95% confidence level, relative to the simulated climate variability. However, the shapes of minimum and maximum temperature PDFs are not predicted to change between 1970-2000 and 2060-2090 under this emission scenario (i.e., the temperature PDFs are simply shifted towards higher temperatures).

No statistically significant change in average rainfall was predicted by the CCAM simulations at the 95% confidence level.

Uncertainties in the GCM simulation and emission scenario have not been quantified in this report (see e.g., CSIRO 2007). Estimating such uncertainties at the regional scale is likely to require an ensemble of dynamical downscaling simulations from which an appropriate statistical analysis could be performed.

However, processing such an ensemble of GCM's and emission scenarios would require a substantial amount of resources for computation and storage.

5. ACKNOWLEDGEMENTS

The authors wish to thank Kim Nguyen, Jack Katzfey and Suppiah Ramasamy for their advice during the writing of this manuscript.

6. REFERENCES

Chouinard, C., Beland, M. and McFarlane, N., 1986. A simple gravity wave drag parametrization for use in medium-range weather forecast models. Atmos.-Ocean, 24, 91-110.

CSIRO, 2007. Climate Change in Australia. CSIRO Marine and Atmospheric Research Technical Report. http://www.climatechangeinaustralia.gov.au/resources.php

Gordon, H. B., Rotstayn, L. D., McGregor, J. L., Dix, M. R., Kowalczyk, E. A., O'Farrell, S. P., 2002. The CSIRO Mk3 climate system model. CSIRO Marine and Atmospheric Research Technical Report 60. http://www.cmar.csiro.au/e-print/open/gordon_2002a.pdf

Holtslag, A. and Boville, B., 1993. Local versus non-local boundary layer diffusion in a global climate model. J. Climate, 6, 1825-1842.

IPCC, 2007. www.grida.no/climate/ipcc/emission/094.htm

Kowalczyk, E.A., Garratt, J.R. and Krummel, P.B., 1994. Implementation of a soil-canopy scheme into the CSIRO GCM – Regional aspects of the model response. CSIRO Marine and Atmospheric Research Technical Report 32. http://www.cmar.csiro.au/e-print/open/kowalczyk_1994a.pdf

McGregor, J. L., 2003. A new convection scheme using a simple closure. BMRC Research Report 75, 43-48.

McGregor, J. L., 2005. C-CAM: Geometric aspects and dynamical formulation. CSIRO Marine and Atmospheric Research Technical Report 70. http://www.cmar.csiro.au/e-print/open/mcgregor_2005a.pdf

McGregor, J. L., and Dix, M. R., 2008. An updated description of the conformal-cubic atmospheric model. High Resolution Simulation of the Atmosphere and Ocean, Hamilton, K. and Ohfuchi, W., Eds., Springer, 51-76.

McGregor, J. L., Gordon, H. B., Watterson, I. G., Dix, M. R., and Rotstayn, L. D., 1993. The CSIRO 9-level Atmospheric General Circulation Model. CSIRO Marine and Atmospheric Research Technical Report 26. http://www.cmar.csiro.au/e-print/open/mcgregor_1993a.pdf

Nguyen, K., and McGregor, 2008. (in preparation)

Rotstayn, L. D., 1997. A physically based scheme for the treatment of stratiform clouds and precipitation in large-scale models. I: Description and evaluation of the microphysical processes. Quart. J. Roy. Meteor. Soc., 123, 1227-1282.

Thatcher, M.J., McGregor, J.L, and Nguyen, K., 2007. Regional climate downscaling for the Marine and Tropical Sciences Research Facility (MTSRF) between 1971-2000. CSIRO Marine and Atmospheric Research report (restricted access)

Thatcher, M.J., McGregor, J.L., 2008. Using a scale-selective filter for dynamical downscaling with the Conformal Cubic Atmospheric Model. Submitted to Mon. Wea. Rev.

Schmidt, F., 1977. Variable fine mesh in spectral global models. Beitr. Phys. Atmos., 50, 211-217.

Schwarzkopf M. D. and Fels, S. B., 1991. The simplified exchange method revisited: an accurate, rapid method for computation of infrared cooling rates and fluxes. J. Geophys. Res., 96, 9075-9096.

Smith, R. N. B., 1990. A scheme for prediction layer clouds and their water content in a general circulation model. Quart. J. Roy. Meteor. Soc., 116, 435-460.